Conformations of Trimethoxymethylsilane: Matrix Isolation Infrared and Ab Initio Studies

V. Kavitha, K. Sundararajan, and K. S. Viswanathan*

Materials Chemistry Division, Indira Gandhi Centre for Atomic Research, Kalpakkam, 603 102 India

Received: April 21, 2005; In Final Form: August 20, 2005

Conformations of trimethoxymethylsilane were studied using matrix isolation infrared spectroscopy and ab initio computations. Trimethoxymethylsilane was trapped in both argon and nitrogen matrixes using heated nozzle effusive sources and a supersonic jet source, in an effort to alter the conformational population in the matrix. Ab initio calculations were carried out at the HF and B3LYP level using 6-31++G** basis set to support our experimental observations. The frequencies computed at the B3LYP level was found to fit well with our experimental data. A conformer with a $C_1(g^{\pm}g^{\pm}t)$ structure was predicted by our computations to be the ground state conformer.

Introduction

Anomeric effect has received considerable attention because of its importance in determining structure, conformational energies, and reactivity in organic compounds. In particular, the anomeric effect at a carbon attached to two oxygen atoms has been extensively studied both experimentally and theoretically.[1−7] For example, in simple systems such as dimethoxymethane, the structure of the ground state conformer is decided by anomeric interactions and has been shown to be gauche−gauche.[5−7] Likewise, anomeric interactions also decide the reactivity in the hydrolysis of acetal and ortho esters, the reactivity being largely determined by the lone pair alignment with respect to the leaving group.[1,8,9] The anomeric effect has also been observed in molecules of the type $CH_2(XH)_2$ where X = S, Se, Te. The magnitude of orbital interactions is less for these elements compared with oxygen; hence, the anomeric effect would be less on substituting sulfur for oxygen and would progressively decrease as we go to Te.[2,10] However, even with Te, the anomeric effect, though less, is still observable.

The extent of anomeric interaction when C is replaced by elements such as Si has not been studied in great detail. Only a few theoretical studies on systems with a central atom other than carbon are available in the literature.[11−14] These studies conclude that the anomeric effect at Si is less than that at C. However, experimental data on these systems are sparse. Electron diffraction study on the structure of trimethoxymethylsilane by Gergö et al.[15] indicated a conformer with C_3 symmetry to be the most stable. However, the possible operation of anomeric effect was not discussed.

In this paper we present our results on matrix isolation infrared and ab initio studies of the conformations of trimethoxymethylsilane (TMMS), to understand the operation of the anomeric effect in silicon compounds. In addition to the interest the Si compounds elicit from the point of view of a basic understanding of the phenomenon of anomeric effect, the alkoxysilanes have commercial importance as these compounds serve as precursors to high molecular weight polymers. Trialkoxysilanes, in particular TMMS, tetraethoxysilane, and triethoxymethylsilane are used to consolidate stone. A good understanding of the molecular structure of these compounds is therefore important and forms the theme of this work.

* To whom correspondence should be addressed. E-mail: vish@igcar.ernet.in.

Experimental Section

Matrix isolation experiments were carried out using a Leybold AG closed cycle compressor cooled cryostat, RD 210. The details of the vacuum system and cryogenics are described elsewhere.[16−18] The sample and matrix gas were mixed in the desired ratio at a typical sample: matrix ratio of 1:2000. The gas mixture was then allowed to stream out of a single-jet effusive nozzle and deposited onto a cold KBr window maintained at temperatures below ∼15 K. The deposition was carried out at a rate of ∼3 mmol h^{-1}, and a typical deposition lasted for ∼1 h. Spectra were recorded using a BOMEM MB 100 FTIR spectrometer with a spectral resolution of 1 cm^{-1} and are referred to as "as deposited spectra". After a spectrum was recorded, the matrix was warmed to 35 K, kept at this temperature for ∼15 min, and recooled to 15 K. The spectra of the matrix thus annealed were also recorded. Experiments were performed by maintaining the effusive source at two different nozzle temperatures, viz. 298 K (room temperature) and 393 K. In the heated nozzle experiments, the nozzle was heated to a length of 35 mm, just prior to the exit of the gas mixture into the vacuum. In addition to performing experiments using an effusive source as described above, we also performed a few experiments using a supersonic jet nozzle to deposit the matrix. For the pulsed supersonic nozzle experiments, a pulsed supersonic nozzle (Parker Hannifin Corporation, USA) was used, with the stagnant pressure of typically 1.3 atm. The pulsed valve was used with a pulse width of 2 ms and a repetition rate of 0.5 Hz in all the experiments. At this deposition rate, the temperature of the cryotip did not rise.

TMMS (97%, Lancaster) was used without any further purification. High-purity argon and nitrogen (Grade INOX-I, Ultrapure) were used as the matrix gas. The spectrum of liquid TMMS, at room temperature, was also recorded using an attenuated total internal reflection (ATR) cell for comparison with the matrix-isolated spectra.

Computational Method

Ab initio molecular orbital calculations were performed using the Gaussian 98W program on an Intel Pentium (R) IV machine.[19] Geometry optimizations were done at both HF and B3LYP levels using 6-31++G** basis set, without imposing any constraints during the optimization process. Vibrational frequency calculations were done at both HF and B3LYP levels using 6-31++G** basis set. The computed frequencies were scaled to bring them into agreement with experimental frequen-

10.1021/jp0520594 CCC: $30.25
Published on Web 09/28/2005

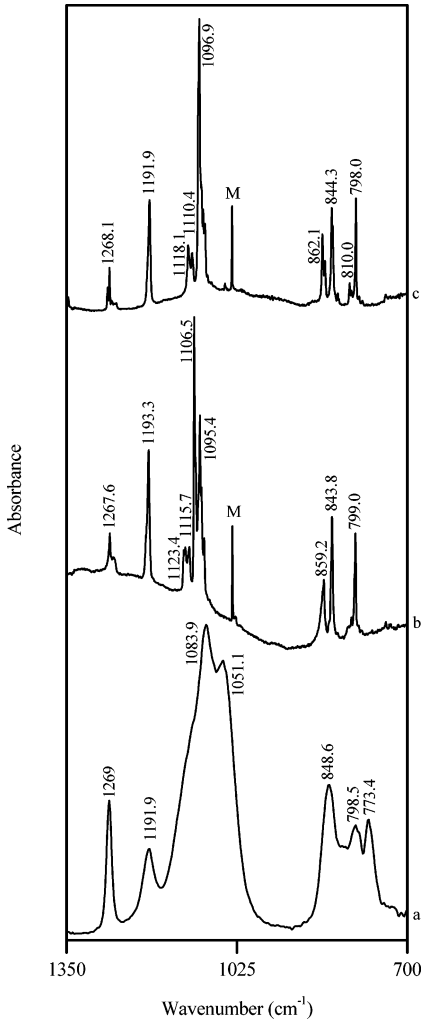

Figure 1. IR spectra of TMMS spanning the region 1350−700 cm^{-1} (a) spectrum of liquid TMMS (at room temperature), (b) matrix isolation infrared spectrum of TMMS in argon, and (c) matrix isolation infrared spectra of TMMS in nitrogen. Spectra shown are in as-deposited matrixes. The spectral feature marked "M" is due to methanol.

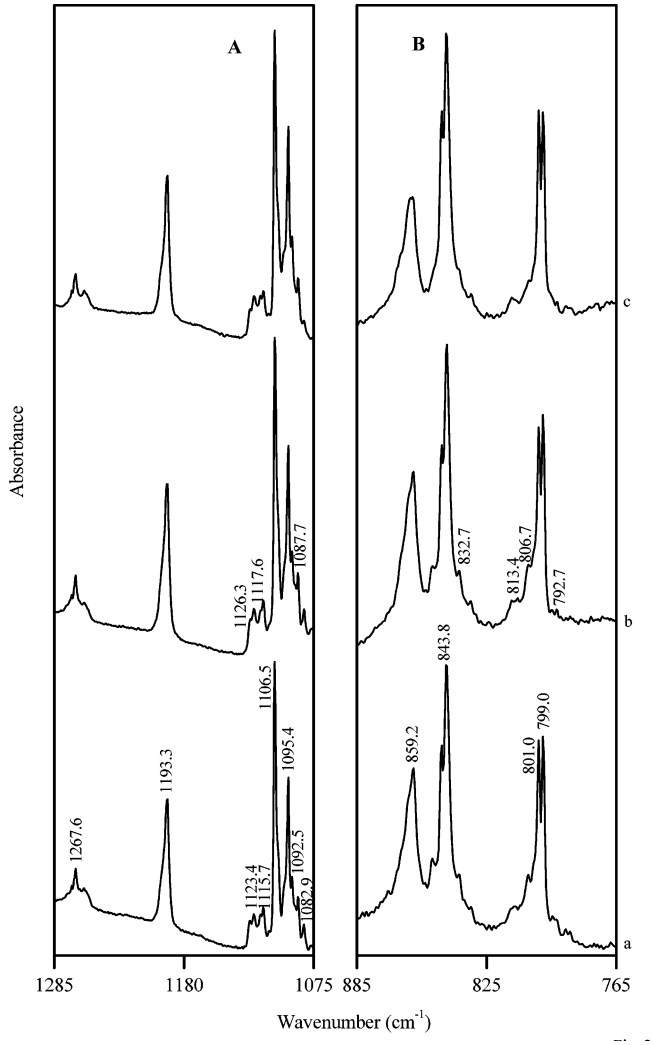

Figure 2. Matrix isolation infrared spectra of TMMS in argon, annealed at 35 K, in the region 1285−1075 cm^{-1} (block A) and in the region 885−765 cm^{-1} (block B). IR spectra of TMMS deposited using (a) an effusive nozzle at room temperature, (b) an effusive nozzle at 393 K, and (c) supersonic nozzle.

cies. To arrive at the scaling factor, the experimentally observed strongest feature (1106.5 cm^{-1}) that could be assigned to the ground state conformer was correlated with that of the strongest computed feature for the ground state conformer. The scaling factor that would bring this computed frequency into agreement with the experimentally observed frequency was calculated and used to scale all other vibrational frequencies. The computed frequencies were used to simulate vibrational spectra using the SYNSPEC program.[20] Vibrational frequency calculations also helped in ascertaining that the computed conformations did indeed correspond to a minimum on the potential surface. Zero-point energies were also calculated. The transition structure connecting the ground state and the higher energy conformer was computed, from which the barrier to conformer interconversion was computed.

Results

Experimental. Figure 1 shows the IR spectra of TMMS trapped in argon and nitrogen matrixes spanning the region 700−1350 cm^{-1}. This region corresponds to the C−O stretching, $SiO-CH_3$ rocking mode of vibrations.[21] Also shown in Figure 1a is the IR spectrum of liquid TMMS. A comparison of the matrix isolated and the liquid spectra reveals the rich resolved features obtained when TMMS is trapped in the cryogenic matrix. The main spectral features of TMMS in the argon matrix (deposited using a room-temperature effusive source) occur at 799.0, 843.8, 859.2, 1095.4, 1106.5, 1193.3, and 1267.6 cm^{-1}. The spectra in the N_2 matrix (Figure 1c) is very similar, though the features, not unexpectedly, are slightly shifted from the argon matrix values.

We then performed experiments with heated nozzle effusive sources. The nozzle temperatures were varied over the temperature range 353−393 K. The idea of these experiments was to alter the conformational population by heating the sample just prior to deposition. Such an exercise proved fruitful in our earlier experiments, such as with dimethoxymethane (DMM)[5] and diethoxymethane (DEM).[22] The features that increase in intensity when the heated nozzle source was used can then be assigned to the higher energy conformers. However, in the case of TMMS, we observed no discernible increase in the intensity of the spectral features, nor were new features seen as the temperature of the nozzle was increased. This observation indicates that, over the temperature range of our experiments, the population of the higher energy conformers did not increase significantly. We then performed experiments with a supersonic jet nozzle to deposit the matrix to look for conformational cooling.

The spectra recorded with the heated effusive sources and supersonic sources are shown in Figure 2. While we have

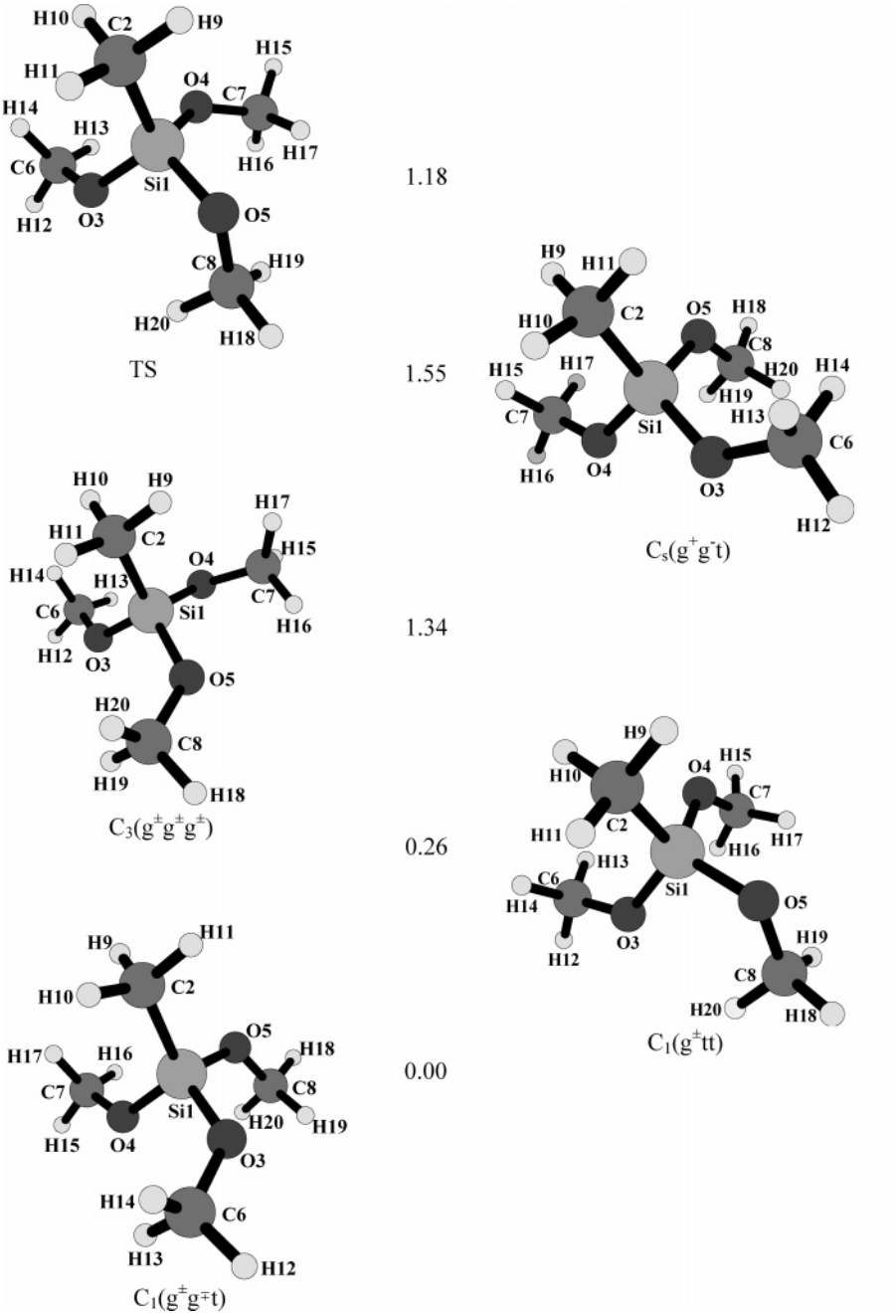

Figure 3. Computed structures of $C_1(g^\pm g^\pm t)$, $C_1(g^\pm tt)$, $C_3(g^\pm g^\pm g^\pm)$, and $C_s(g^+g^-t)$ conformers. The structure of the TS connecting the $C_1(g^\pm g^\pm t)$ and $C_1(g^\pm tt)$ conformer is also shown. Relative energies, in kcal/mol, are given against each structure.

recorded the spectra over the region 4000−400 cm^{-1}, only the regions 1285−1075 and 885−765 cm^{-1} are shown, as these are the regions that carry information on the conformations of TMMS.

Computational. Geometry optimizations were performed at the HF and B3LYP level using 6-31++G** basis set. The optimized structural parameters obtained at the B3LYP/6-31++G** are given in Table 1. The corresponding structures are shown in Figure 3. The structure of the different conformers differs mainly in the dihedral angle between the C−O−Si and O−Si−C planes. At B3LYP level four minima corresponding to $C_1(g^\pm g^\pm t)$, $C_1(g^\pm tt)$, $C_3(g^\pm g^\pm g^\pm)$, and $C_s(g^+g^-t)$ conformers in the order of increasing energy were obtained.[23] Vibrational frequency calculations yielded all-positive frequencies for these conformers, confirming that all these structures were minima on the potential surface. At the HF level, however, only three minima corresponding to $C_1(g^\pm g^\pm t)$, $C_1(g^\pm tt)$, and $C_3(g^\pm g^\pm g^\pm)$ conformers, in order of increasing energy, were obtained. Conformer with the $C_s(g^+g^-t)$ structure was found to be a first-order saddle point at the HF level. The energies of the various conformers at both levels of theory are given in Table 2.

The vibrational frequencies calculated at B3LYP level (and scaled) were found to fit well with the experimental frequencies and hence we have included only these frequencies in Table 3.

Discussion

Vibrational Assignments. The main spectral features at 799.0, 843.8, 859.2, 1095.4, 1106.5, 1193.3, and 1267.6 marked in Figure 2a are essentially those of the ground state conformer, which is indicated by our computations to have a $C_1(g^\pm g^\pm t)$ structure. The computed, scaled frequencies calculated at B3LYP level fit well with our room-temperature effusive source experiment. Both the experimental and computed frequencies are given in Table 3.

TABLE 1: Selected[a] Computed Parameters of TMMS; Bond Distances (Å), Bond Angles (deg), and Torsion Angles[b] (deg) Computed at the B3LYP/6-31++G Level**

parameters	$C_1(g^{\pm}g^{\pm}t)$	TS[c]	TS[d]	$C_1(g^{\pm}tt)$	C_3-$(g^{\pm}g^{\pm}g^{\pm})$	C_s-$(g^{+}g^{-}t)$
C^2-Si^1	1.8647	1.8614	1.8608	1.8591	1.8723	1.8659
O^3-Si^1	1.6533	1.6592	1.6499	1.6665	1.6534	1.6560
O^4-Si^1	1.6655	1.6612	1.6657	1.6611	1.6538	1.6554
O^5-Si^1	1.6526	1.6536	1.6593	1.6516	1.6536	1.6631
C^6-O^3	1.4238	1.4230	1.4239	1.4228	1.4231	1.4218
C^7-O^4	1.4222	1.4209	1.4226	1.4234	1.4232	1.4215
C^8-O^5	1.4264	1.4256	1.4240	1.4241	1.4231	1.4263
$O^3-Si^1-C^2$	113.91	112.62	111.08	113.87	111.23	113.36
$O^4-Si^1-C^2$	111.99	109.52	113.44	106.05	111.28	113.49
$O^5-Si^1-C^2$	106.37	107.95	105.73	109.85	111.23	105.60
$C^6-O^3-Si^1$	126.50	126.19	129.40	124.82	126.23	124.73
$C^7-O^4-Si^1$	125.47	128.75	125.25	124.85	126.08	125.10
$C^8-O^5-Si^1$	124.85	126.13	124.78	128.32	126.13	124.00
$C^6O^3Si^1C^2$	83.38	82.05	129.68	63.09	73.61	−59.48
$C^7O^4Si^1C^2$	55.72	114.38	62.04	169.82	72.00	56.63
$C^8O^5Si^1C^2$	170.66	158.14	168.12	143.78	72.09	−180.38
$C^6O^3Si^1O^4$	−39.27	−38.96	6.77	−55.87	−48.45	178.21
$O^3Si^1O^4C^7$	179.60	−122.7 1	−176.5 9	−66.54	−165.98	178.84
$C^8O^5Si^1O^3$	48.23	36.730	47.58	21.01	−50.07	56.21

[a] The complete geometry in Cartesian coordinates for all the conformers and the transition states are presented as Supporting Information. [b] Torsional angles of the fragment ABCD denotes the angle between ABC and BCD planes. [c] TS connecting $C_1(g^{\pm}g^{\pm}t)$ and $C_1(g^{\pm}tt)$. [d] TS connecting $C_1(g^{\pm}g^{\pm}t)$ and $C_1(tg^{\pm}t)$.

TABLE 2: Zero-Point Vibrational Energies (Hartrees), Relative Energies (kcal/mol), and Dipole Moment (D) of $C_1(g^{\pm}g^{\pm}t)$, $C_1(g^{\pm}tt)$, $C_3(g^{\pm}g^{\pm}g^{\pm})$, and $C_s(g^{+}g^{-}t)$ Conformers of TMMS

conformer	degeneracy	ZPE scaled (Hartrees)		relative energy ZPE corrected (kcal/mol)		dipole moment	
		HF[a]	B3LYP[b]	HF	B3LYP	HF	B3LYP
$C_1(g^{\pm}g^{\pm}t)$	6	0.1580383	0.1633219	0.00[c]	0.00[d]	1.3	1.3
$C_1(g^{\pm}tt)$	6	0.1583016	0.1633021	0.25	0.27	1.6	1.5
$C_3(g^{\pm}g^{\pm}g^{\pm})$	2	0.1581920	0.1630320	1.13	1.34	0.8	1.3
$C_s(g^{+}g^{-}t)$	3		0.1631576		1.55		1.2
TS[e]			0.1631636		1.08		1.2
TS[f]			0.1632550		0.24		1.5

[a] Scaling factor 0.8989. [b] Scaling factor 0.9895. [c] Absolute energy of the ground state conformer, without ZPE correction, is −672.1201725 Hartrees at the HF level. [d] Absolute energy of the ground state conformer, without ZPE correction, is −674.9673062 Hartrees at the B3LYP level. [e] TS connecting $C_1(g^{\pm}g^{\pm}t)$ and $C_1(g^{\pm}tt)$. [f] TS connecting $C_1(g^{\pm}g^{\pm}t)$ and $C_1(tg^{\pm}t)$.

The first higher energy conformer, $C_1(g^{\pm}tt)$, lies 0.27 kcal/mol above the ground state conformer. At room temperature the contribution of the $C_1(g^{\pm}g^{\pm}t)$ and $C_1(g^{\pm}tt)$ to the overall population would be in the ratio 58.2:37.6, computed using the energies and degeneracies shown in Table 2. The contribution of the higher energy conformer, $C_1(g^{\pm}tt)$, to the overall population in the matrix at 12 K cannot be ruled out, a discussion of which is presented later. However, it is difficult to resolve the features of the $C_1(g^{\pm}g^{\pm}t)$ and $C_1(g^{\pm}tt)$ conformers, as their vibrational frequencies are very close to each other. The observed features in Figure 2 are probably due to both the conformers. At 393 K, the contribution of the two conformers would be in the ratio 54.1:38.8, which is only slightly different from the ratio at room temperature. It is therefore not surprising that when the heated nozzle source was used, no significant changes in the spectra were observed.

We then performed supersonic nozzle experiments in an attempt to depopulate the higher energy $C_1(g^{\pm}tt)$ conformer. The as-deposited spectrum obtained with a supersonic jet source was somewhat different from that obtained with an effusive source; however, on annealing the matrix, the two spectra were similar (Figure 2). This indicates that the minor differences observed in the as-deposited spectrum with a supersonic jet source were probably due to site effects, which probably was washed away during annealing. Manifestation of site effects with different deposition sources is not surprising. As mentioned earlier, both $C_1(g^{\pm}g^{\pm}t)$ and $C_1(g^{\pm}tt)$ conformers may contribute to the spectra; however, with both our heated nozzle effusive source and the supersonic nozzle source we could not unambiguously resolve the features due to the two conformers. The spectral assignments of various vibrational modes are given in Table 3. In Figure 4 we show the synthetic spectra of TMMS obtained by adding the computed spectra of the two conformers, $C_1(g^{\pm}g^{\pm}t)$ and $C_1(g^{\pm}tt)$, weighted for their relative populations at room temperature and it can be seen to compare well with the experimental spectra obtained at room temperature, using an effusive source.

The two conformers with $C_3(g^{\pm}g^{\pm}g^{\pm})$ and $C_s(g^{+}g^{-}t)$ structures lie 1.34 and 1.55 kcal/mol above the ground state conformer, respectively. Together these conformers contribute less than 5% to the overall population and hence have been neglected in all discussions on vibrational assignments.

We have computed the transition states connecting $C_1(g^{\pm}g^{\pm}t)$ and $C_1(g^{\pm}tt)$ conformer at B3LYP/6-31++G** level. There can be two pathways connecting $C_1(g^{+}g^{+}t)$ and $C_1(g^{+}tt)$ conformers, where either of the two gauche carbons (g) can be rotated to adopt the trans (t) orientation. Both the transition states were located and confirmed through frequency calculations to be first-order saddle points. An examination of the normal mode of the imaginary frequency indicates it to correspond to a rotation around the Si−O bond in question. The barrier for the conformer interconversion of the $C_1(g^{\pm}tt)$ structure to the $C_1(g^{\pm}g^{\pm}t)$ form was found to be extremely small or even near-barrierless, at the level of computations that we used. These computations

TABLE 3: Experimental Vibrational Frequencies in Argon and Nitrogen Matrixes and Computed Scaled Frequencies[a] of $C_1(g^{\pm}g^{\pm}t)$ and $C_1(g^{\pm}tt)$ Conformers of TMMS, Computed at the B3LYP/6-31++G Level; Intensities Are Given in Parentheses**

mode[b]	$C_1(g^{\pm}g^{\pm}t)$	$C_1(g^{\pm}tt)$	experimental	
			argon	nitrogen
Si−C stretch	782.2 (118)	789.4 (102)	799.0, 806.3	798.0, 810.0
	843.9 (150)	843.0 (153)	843.8	844.3
	861.2 (148)	858.9 (153)	859.2	856.8, 862.1
O−C stretch	1104.3 (339)	1101.0 (265)	1087.7, 1095.4	1086.3, 1089.5
	1106.5 (377)	1105.7 (309)	1106.5	1096.9
	1122.4 (135)	1125.8 (242)	1115.7, 1123.4	1110.4, 1118.1
O−CH_3 rocking	1193.8 (67)	1192.8 (54)	1193.3	1191.9
	1194.5 (69)	1194.3 (59)		
H−C−H bending (in Si−CH_3)	1295.6 (50)		1259.4, 1267.6	1268.1, 1271.4
OC−H stretch	2979.9 (80)	2980.7 (72)	no firm assignments made	
	2986.3 (82)	2981.6 (59)		
	2991.2 (62)	2990.9 (91)		

[a] Scaling factor used was 0.9895. [b] Approximate mode assignments based on ref 21 and vibrational visualization program GaussView 2.1.

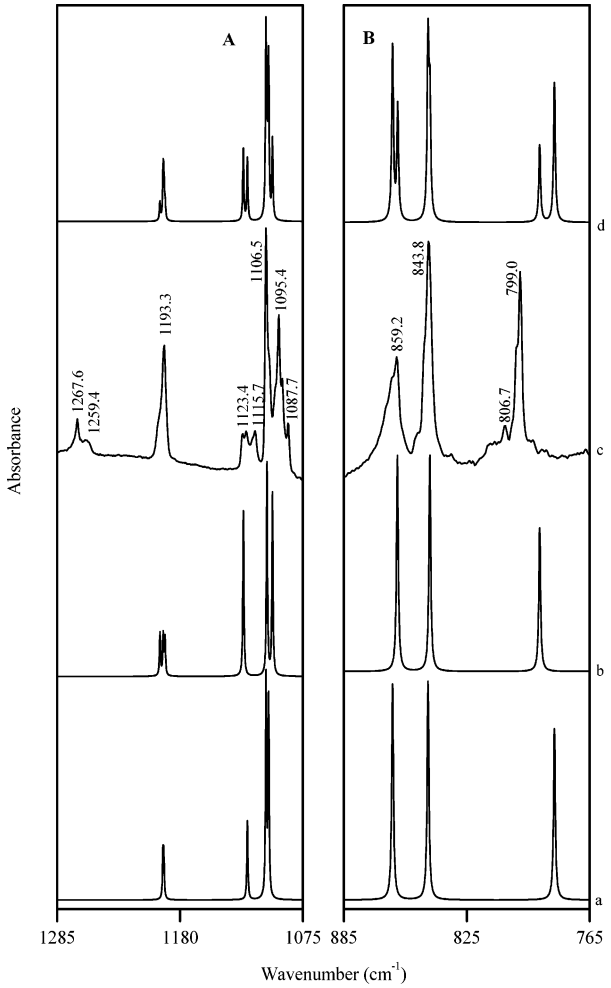

Figure 4. Matrix isolation infrared spectra of TMMS in argon in the region 1285−1075 cm^{-1} (block A) and in the region 885−765 cm^{-1} (block B). (a) Computed spectra of $C_1(g^{\pm}g^{\pm}t)$ conformer, (b) computed spectra of $C_1(g^{\pm}tt)$ conformer, (c) IR spectra of as-deposited matrix deposited using a room-temperature effusive source, and (d) computed spectra obtained by adding spectra of $C_1(g^{\pm}g^{\pm}t)$ and $C_1(g^{\pm}tt)$ conformers, weighted for their respective populations.

therefore imply a facile conformer interconversion. However, it must be remembered that these computed barriers are for the free molecule, and in the matrix, where the molecule experiences a cage effect, these barriers may be higher. Hence, quenching of the room-temperature population distribution, in the 12 K matrix, cannot be ruled out. It is for this reason that we have taken into consideration both the $C_1(g^{\pm}g^{\pm}t)$ and $C_1(g^{\pm}tt)$ conformers when making vibrational assignments. In a supersonic expansion, however, where no such extraneous (matrix) barrier exists, the computed free molecule barriers must be applicable, and we should expect to see conformational cooling for such low barriers. Unfortunately, TMMS does not have features that can be uniquely assigned to the two conformers, to unambiguously check such a possibility.

Dipole Moment. The dipole moments of the conformers of TMMS were given in Table 2. It can be seen from the table that the dipole moments of the different conformers are only slightly different from each other, with the lowest energy conformer, $C_1(g^{\pm}g^{\pm}t)$, having a dipole moment of 1.3 D. The $C_1(g^{\pm}tt)$ conformer was computed to have a dipole moment of 1.5 D, the highest among all the conformers. The net dipole moment of TMMS, weighted for the populations of all the four conformers, was computed to be 1.38 D. There were no reported data on the dipole moment measurements on TMMS for comparison.

Conclusions

We have recorded the infrared spectra of TMMS trapped in both argon and nitrogen matrixes. Supported by ab initio computations at the B3LYP/6-31++G** level, we assigned the features to various vibrational modes of TMMS. The experimentally obtained spectra were assigned to the conformers with $C_1(g^{\pm}g^{\pm}t)$ and $C_1(g^{\pm}tt)$ structures, which our computations indicated to be the lowest energy and the first higher energy forms. This conclusion is in variance with that of Gergö et al.[15] who had indicated a conformer with a C_3 symmetry to be the ground state. However, they had constrained their analysis to only conformers with C_3 geometries and their search was therefore not global. Conformers with energies higher than the two mentioned above, such as a $C_3(g^{\pm}g^{\pm}g^{\pm})$, were also located on the potential surface, but would have very little population at room temperature to be of any experimental significance. This study represents the first detailed report on the conformations of methoxysilanes. The anomeric effect probably leads to the "$g^{\pm}g^{\pm}t$" conformer to be the ground state. Further work on related silicon compounds will be required to understand in detail the operation of the anomeric effect in these compounds.

Acknowledgment. V.K. gratefully acknowledges the grant of a research fellowship from the Council of Scientific and Industrial Research (CSIR), India.We also thank the reviewers for their critical comments.

Supporting Information Available: Optimized geometries in Cartesian coordinates of the various conformers and transition states of TMMS. This material is available free of charge via the Internet at http://pubs.acs.org.

References and Notes

(1) Thatcher, G. R. J. Anomeric effect and associated stereoelectronic effects; ACS Symposium Series 539; American Chemical Society: Washington, DC, 1993.

(2) Schleyer, P. v. R.; Jemmis, E. D.; Spitznagel, G. W. *J. Am. Chem. Soc.* **1985**, *107*, 6393.

(3) Aliette, C.-B.; Jacques-Emile, D. *J. Am. Chem. Soc.* **1987**, *109*, 1503.

(4) Aped, P.; Apeliog, Y.; Ellencweig, A.; Fuchs, B.; Goldberg, I.; Karni, M.; Tartakovsky, E. *J. Am. Chem. Soc.* **1987**, *109*, 1486.

(5) Venkatesan, V.; Sundararajan, K.; Sankaran, K.; Viswanathan, K. S. *Spectrochim. Acta Part A* **2002**, *58*, 467.

(6) Wiberg, K. B.; Murcko, M. A. *J. Am. Chem. Soc.* **1989**, *111*, 4821.

(7) Smith, G. D.; Jaffe, R. L.; Yoon, D. Y. *J. Phys. Chem.* **1994**, *98*, 9072.

(8) Li, S.; Dory, Y. L.; Deslongchamps, P. *Tetrahedron* **1996**, *52*, 14841.

(9) Deslongchamps, P.; Dory, Y. L.; Li, S. *Tetrahedron* **2000**, *56*, 3533.

(10) Salzner, U.; Schleyer, P. v. R. *J. Am. Chem. Soc*, **1993**, *115*, 10231.

(11) Reed, A. E.; Schleyer, P. v. R. *J. Am. Chem. Soc.* **1987**, *109*, 7362.

(12) Reed, A. E.; Schleyer, P. v. R. *Inorg. Chem*, **1988**, *27*, 3969.

(13) Pavan Kumar, P. N. V.; Wang, D.-X.; Lam, B.; Albright, T. A.; Jemmis, E. D. *J. Mol. Struct.* **1989**, *194*, 183.

(14) Apeloig, Y.; Stanger, A. *J. Organomet. Chem.* **1988**, *346*, 305.

(15) Gergö, É.; Hargittai, I.; Schultz, G. Y. *J. Organomet. Chem.* **1976**, *112*, 29.

(16) George, L.; Sankaran, K.; Viswanathan, K. S.; Mathews, C. K. *Appl. Spectrosc*. **1994**, *48*, 7.

(17) Vidya, V.; Sankaran, K.; Viswanathan, K. S. *Chem. Phys. Lett.* **1996**, *258*, 113.

(18) George, L.; Viswanathan, K. S.; Singh, S. *J. Phys. Chem. A* **1997**, *101*, 2459.

(19) Frisch, M. J.; Trucks, G. W.; Schlegel, H. B.; Scuseria, G. E.; Robb, M. A.; Cheeseman, J. R.; Zakrzewski, V. G.; Montgomery Jr., J. A.; Stratmann, R. E.; Burant, J. C.; Dapprich, S.; Millam, J. M.; Daniels, A. D.; Kudin, K. N.; Strain, M. C.; Farkas, O.; Tomasi, J.; Barone, V.; Cossi, M.; Cammi, R.; Mennucci, B.; Pomelli, C.; Adamo, C.; Clifford, S.; Ochterski, J.; Petersson, G. A.; Ayala, P. Y.; Cui, Q.; Morokuma, K.; Malick, D. K.; Rabuck, A. D.; Raghavachari, K.; Foresman, J. B.; Cioslowski, J.; Ortiz, J. V.; Baboul, A. G.; Stefanov, B. B.; Liu, G.; Liashenko, A.; Piskorz, P.; Komaromi, I.; Gomperts, R.; Martin, R. L.; Fox, D. J.; Keith, T.; Al-Laham, M. A.; Peng, C. Y.; Nanayakkara, A.; Challacombe, M.; Gill, P. M. W.; Johnson, B.; Chen, W.; Wong, M. W.; Andres, J. L.; Gonzalez, C.; Head-Gordon, M.; Replogle, E. S.; and Pople, J. A. *Gaussian 98*, Revision A.9; Gaussian, Inc.: Pittsburgh, PA, 1998.

(20) The spectra were simulated using SYNSPEC made available by Irikura, K. National Institute of Standards and Technology: Gaithersburg, MD, 1995.

(21) Smith, A. L. *Spectrochim. Acta* **1960**, *16*, 87.

(22) Venkatesan, V.; Sundararajan, K.; Viswanathan, K. S. *J. Phys. Chem A* **2002**, *106*, 7707.

(23) The notation "g" refers to a gauche orientation of the carbon atoms, C6, C7, C8 with respect to C2; for example, the dihedral angle between planes $C^6O^3Si^1$ and $O^3S^1C^2$ in the ground state conformer is 83.4° and hence is referred to as gauche. If the same dihedral angle is near 180°, it is referred to as "t" (trans).